

John R. de Bruyn

## Transient and steady-state drag in foam

Received: 18 March 2004  
Accepted: 21 May 2004  
Published online: 28 September 2004  
© Springer-Verlag 2004

J. R. de Bruyn  
Department of Physics and Physical  
Oceanography, Memorial University of  
Newfoundland, St. John's, Newfoundland,  
A1B 3X7, Canada

J. R. de Bruyn  
Laboratoire de Rhéologie,  
Domaine Universitaire, B.P. 53, 38041  
Grenoble Cedex 9, France  
E-mail: jdebruyn@ujf-grenoble.fr  
Tel.: +33-0476-825177  
Fax: +33-0476-825164

**Abstract** The steady-state force exerted on a sphere moving at constant speed through an aqueous foam is studied experimentally. The dependence of the force on container size indicates that the moving sphere is surrounded by a fluidised region that extends approximately one sphere radius into the foam. The force increases with the speed of the sphere, but with a finite zero-speed intercept which is a measure of the yield stress of the foam. The steady-state force as a function of pulling speed yields a flow curve which can be described by a Herschel-Bulkley constitutive relation. The transient build-up of

the force when motion starts, and its relaxation when motion stops, are also studied. While the initial build-up has a single time constant inversely proportional to the imposed shear rate, the relaxation involves three distinct processes which we relate to events on the scale of the individual bubbles making up the foam.

**Keywords** Foam rheology · Drag force · Wall effects · Yield-stress fluids · Stress relaxation

### Introduction

Aqueous foams find widespread application in areas as diverse as fire fighting, oil recovery, and shaving. Their utility stems largely from their complex rheological properties (Heller and Kuntamukkula 1987; Kraynik 1988; Weaire and Hutzler 2001). Aqueous foams are composed of many bubbles of gas in a continuous water-based liquid phase, and their properties result from their small-scale structure: the surface tension of the bubbles leads to an elastic response to small applied stresses, but at high stress the bubbles can rearrange themselves to accommodate bulk flow. As a result, foams have a yield stress  $\sigma_y$ , below which they behave like a soft elastic solid. For applied stresses larger than  $\sigma_y$  they flow, but with a viscosity that decreases with shear rate. Although foam rheology has been of interest for some time (Heller

and Kuntamukkula 1987; Kraynik 1988), a detailed understanding of foam behaviour in terms of bubble-scale structure and dynamics has only recently begun to develop. This is largely due to experiments that use multiply-scattered light to probe the bubble-scale behaviour, in combination with rheological studies of bulk flow properties (Cohen-Addad and Höhler 2001; Durian et al 1991a, 1991b; Gopal and Durian 1995, 1999, 2003). Models have been developed which elucidate details of foam structure, flow in response to applied shear, and coarsening (Bolton and Weaire 1990; Durian 1995, 1997; Kabla and Debrégeas 2003; Khan and Armstrong 1986; Kraynik 1988; Okuzono and Kawasaki 1995; Tewari et al 1999; Princen 1983; Reinelt and Kraynik 1990).

This paper concerns the drag force  $F$  exerted on a sphere being pulled through an aqueous foam. For slow

motion of a sphere through a Newtonian fluid, Stokes' Law gives a drag force proportional to the speed  $v$ :  $F = -6\pi\eta r v$ , where  $r$  is the sphere radius and  $\eta$  is the viscosity. The velocity field induced in the fluid by the moving sphere falls off as one over the distance from the sphere (Happel and Brenner 1965). In a yield-stress fluid, however, the material is sheared only where the local stress  $\sigma$  exceeds the yield stress. A moving object is therefore surrounded by a fluidised sheared region in which  $\sigma > \sigma_y$ , while outside this region  $\sigma < \sigma_y$  and the material remains unshaped and solid-like (Atapattu et al 1990, 1995; Beaulne and Mitsoulis 1997; Beris et al 1985; Blackery and Mitsoulis 1997; Deglo De Besses et al 2004). The motion of slowly-moving spheres in yield-stress fluids has been studied experimentally using materials such as Carbopol, a transparent polymer dispersion (Atapattu et al 1990, 1995; Hariharaputhrian et al 1998; Jossic and Magnin 2001), as well as theoretically and numerically (Beris et al 1985; Beaulne and Mitsoulis 1997; Blackery and Mitsoulis 1997; Deglo De Besses et al 2004).

In this paper we study the both the steady-state drag force on a sphere moving through an aqueous foam, as well as the transient build-up and relaxation of the force when motion starts and stops. Our results provide information about both the bulk foam rheology and the local bubble-scale dynamics within the material.

## Experimental

We studied the force exerted by a foam on a steel ball while and after it was pulled vertically upwards at constant speed through the foam. The foam used was Gillette Foamy Regular, a commercial shaving foam which has been used in previous studies of foam behaviour (Durian et al 1991a, 1991b; Gopal and Durian 1995, 1999, 2003; Cohen-Addad and Höhler 2001). It consists of 92% (by volume) tightly packed, polydisperse gas bubbles in an aqueous solution containing steric acid and triethanolamine. The foam coarsens as it ages. Durian et al (1991b) found that the mean bubble diameter in this material was approximately constant at about 30  $\mu\text{m}$  for freshly produced foam. After the foam has aged for about 20 min, the mean bubble diameter starts to increase with a power law dependence on time, reaching 60  $\mu\text{m}$  for foam that has aged for 100 min.

A steel ball of diameter  $d = 2.54$  cm, much larger than the bubble size, was connected to a calibrated load cell by a length of fine nylon thread epoxied to the top of the ball. The ball was pulled upwards at constant speed through a column of foam by a computer-controlled stepper motor driving a linear motion actuator. A computer program allowed control of the speed and duration of the motion and recorded the force data at regular, pre-programmed intervals for later analysis.

Prior to each run, the steel ball was positioned approximately three ball diameters up from the bottom of a vertical Plexiglas tube, closed at the bottom, of inside diameter  $D$  and height 38.5 cm. Seven different tubes were used, with  $D$  ranging from 2.86–8.57 cm, corresponding to  $1.125 \leq D/d \leq 3.375$ . The tube was completely filled with foam injected via a length of plastic tubing through two holes drilled in the tube wall, one slightly above and one slightly below the ball. These holes were then plugged with rubber stoppers cut so as not to protrude into the tube. Care was taken to avoid the presence of large voids in the foam; this was usually not a problem as long as the can of foam being used was relatively full. After the tube was filled, the foam was allowed to relax for two minutes before the run was started. The tubes were used without any surface treatment. At a given height, some downward backflow of the foam at the walls was observed as the ball moved upward through that height, indicating that wall slip was significant. It was particularly pronounced for the smaller tubes. Its presence does not change the general conclusions drawn from this work but does affect the quantitative values of the forces measured.

A typical run involved pulling the ball upwards at a set speed  $v$  for a set time, typically 10–50 s. The ball was then stopped for a longer period, normally 1200 s. This cycle was then repeated a number of times as the foam aged. Speeds in the range  $0.0127 \leq v \leq 1.02$  cm/s were used. The ball remained centred in the tube throughout the experiment. The force measured by the load cell was recorded throughout. The duration of a run – that is, the number of cycles – was limited by the length of the foam column and the need to avoid end effects as the ball approached the top, as well as by aging of the foam. Normally a run included five cycles, but runs at high  $v$  had fewer cycles while some runs at low pulling speeds were continued for up to 40 cycles. The age dependence of our results will be discussed elsewhere. Here we focus on the behaviour of the drag force for “fresh” foam – for the first cycle of pulling and relaxation. The age of our foam is therefore about 120 s at the start of the cycle and 1330–1380 s at the end. In this regime the mean bubble diameter remains roughly constant; our foams are not yet in the regime of power law coarsening studied by Durian et al (1991b).

## Results

Figure 1 shows the measured force as a function of time for the first cycle of a typical run. Later cycles are similar, but, as will be discussed elsewhere, the magnitude of the drag force decreases and the timescales for both the onset and the relaxation of the drag change systematically as the foam ages (de Bruyn, unpublished work). When the ball is put in motion, the drag force

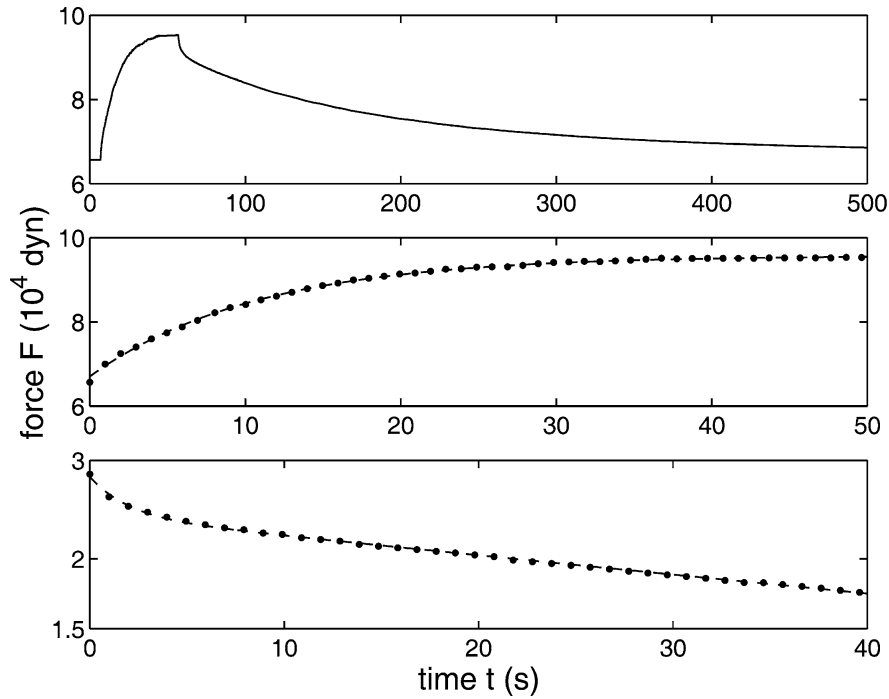


**Fig. 1** Top: A plot of the measured force as a function of time for one cycle of a run with  $D/d=2.25$ . The ball is pulled upwards with speed  $v=0.0254$  cm/s for 50 s, then stopped. The system then relaxes for 1200 s; only the first 450 s of the relaxation segment are shown. Middle: The portion of the top graph for which the ball is moving, showing the build-up of the drag force to a steady-state value. Only every third data point is shown for clarity. The dashed line is a fit to a single exponential approach to a constant force, as described in the text. Bottom: A semi-log graph of the first 40 s of the relaxation segment of the top graph with the constant offset force  $F_1$  subtracted. The relaxation of the force is non-exponential; an initial rapid drop is followed by a much slower decay. Only every third data point is shown. The dashed line is a fit to the sum of three decaying exponentials as described in the text

builds up to a steady-state value with a timescale of a few seconds. When the motion is stopped, there is an initial rapid drop in the force, after which the remaining force relaxes over a much longer timescale of the order of several hundred seconds. For comparison, data taken with the same apparatus using corn syrup, a Newtonian fluid, show the expected instantaneous response – the drag force immediately jumps to its steady state value when the ball starts to move, and returns immediately to its original value when the motion stops.

The approach of the drag force to its steady-state value is shown on an expanded scale in the middle graph of Fig. 1. This transient build-up of the force is well described by an exponential function of time  $t$  of the form

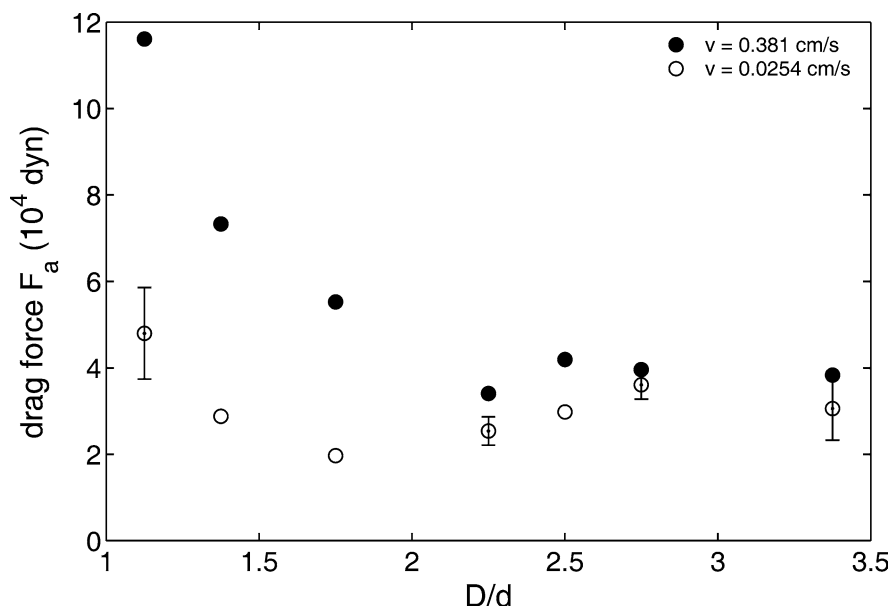
$$F(t) = F_a \left(1 - e^{-t/\tau_a}\right) + F_0, \quad (1)$$

where  $F$  is the total measured force,  $F_0$  is the initial force measured before the ball starts to move upwards,  $F_a$  is

the steady state drag force, and  $\tau_a$  is a time constant. A fit to this expression is shown as a dashed line in the middle graph of Fig. 1. From similar fits to a number of runs we determined the parameters  $F_a$ ,  $\tau_a$ , and  $F_0$  as functions of pulling speed  $v$  and tube size  $D$ .

Figure 2 shows  $F_a$ , the steady-state drag force for fresh foam, plotted as a function of tube size for two different pulling speeds. For a speed of 0.381 cm/s (solid circles) the steady state drag is constant within the experimental scatter for  $D/d \gtrsim 2$  but increases substantially for smaller tubes. For a lower speed, the variation of  $F_a$  with  $D/d$  is similar but less pronounced, with a significant increase in  $F_a$  occurring only for the smallest tubes. (The minimum in the force observed for the low-speed data is probably not significant; it is not present in the data for the same foam at later times.) These results indicate that the walls of the tube have no effect on the drag for large enough tubes. Since the foam has a yield stress, it remains unsheared outside the fluidised region around the moving sphere. The presence of the walls will have an effect on the drag only if the sheared region extends to the wall of the tube (Atapattu et al 1990), otherwise the flow does not “see” the walls and the container is effectively infinite. Our results for the higher speed indicate that in this case wall effects contribute to the drag for  $d/D \lesssim 2$ ; that is, when the space between the surface of the sphere and the wall is less than the sphere radius  $d/2$ . For the smaller speed, the effect of the walls is not seen for  $D/d \gtrsim 1.5$ , indicating that the sheared region is smaller at lower pulling speeds, consistent with previous numerical results (Beris et al 1985; Deglo De Besses et al 2004).

**Fig. 2** The steady-state drag force  $F_a$  for fresh foam as a function of the ratio of tube size  $D$  to sphere diameter  $d$ . The error bars indicate the range of data obtained from multiple runs under the same conditions. The force is roughly constant for  $D/d \geq 2$  and increases for smaller  $D/d$  as wall effects become important



$F_a$  is plotted as a function of pulling speed for two tube sizes in Fig. 3. Within our scatter,  $F_a$  increases linearly with  $v$ , with the slope being larger for the smaller tube. The drag force has a finite intercept at zero  $v$  which is independent of tube size. Straight-line fits are shown as dashed lines in Fig. 3. Beris et al (1985) found numerically for a sphere in a Bingham fluid that the force  $F_y$  required to overcome the yield stress was given by  $F_y = 14\pi r^2 \sigma_y$ . Using this result, our force intercept of  $37600 \pm 900$  dyn corresponds to a yield stress of  $530 \pm 10$  dyn/cm<sup>2</sup>.

Although the flow in our system is certainly not a simple rheometric flow, we can nonetheless use these data to obtain an approximation to a conventional flow curve in terms of stress  $\sigma$  and shear rate  $\dot{\gamma}$ . We assume the relationship between force and stress found by Beris et al (1985) continues to apply when the sphere is actually moving and use it to convert our force values into stresses:  $\sigma_a = F_a/14\pi r^2$ . To convert pulling speed into shear rate, we note that the flow velocity will go from  $v$  to zero over a distance corresponding to the size of the sheared region. The data shown in Fig. 2 indicate that

**Fig. 3** The steady-state drag force  $F_a$  as a function of pulling speed  $v$  in tubes with two different values of  $D/d$ . The dashed lines are fits to straight lines. Although the slope is higher for the smaller tube, the intercept is independent of tube size

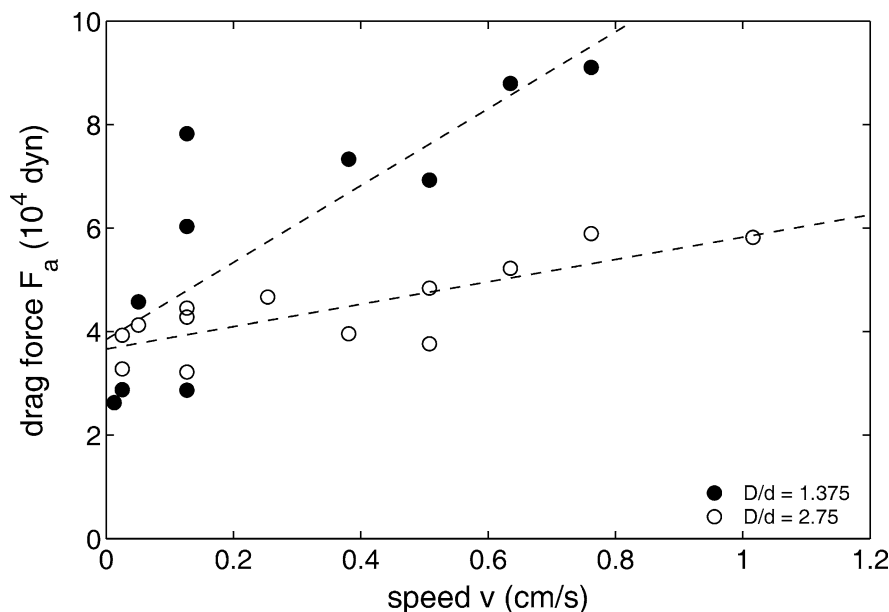
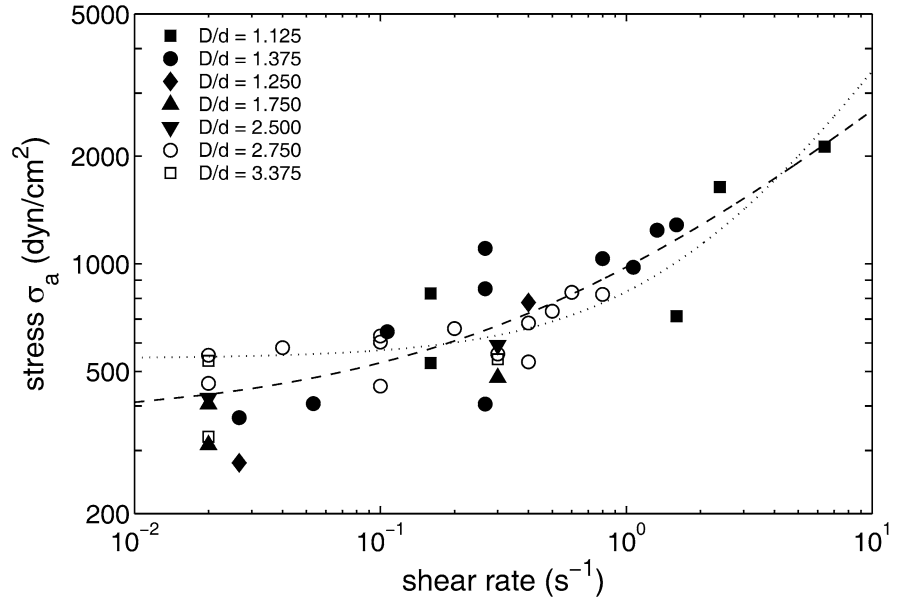


**Fig. 4** Stress  $\sigma_a$  as a function of shear rate  $\dot{\gamma}$ , estimated as discussed in the text. The different symbols indicate data taken with different tube sizes. The dashed line is a fit to the Herschel-Bulkley constitutive relation, and the dotted line a fit to the Bingham constitutive relation, as discussed in the text



this distance is approximately  $d/2$ , and so we use  $\dot{\gamma} \approx 2v/d$  for  $D/d > 2$ . For smaller tubes, as seen above, the sheared region extends out to the tube wall and the relevant distance is that between the surface of the sphere and the wall,  $(D-d)/2$ . We therefore use  $\dot{\gamma} \approx 2v/(D-d)$  for  $D/d < 2$ . The resulting values of stress versus shear rate are plotted for all of our data in Fig. 4. Within the experimental scatter the data collapse onto a single curve, which, as it should be, is a characteristic of the material and independent of tube size. Although the  $F$  versus  $v$  data for the individual tubes plotted in Fig. 3 appeared linear in  $v$ , the data for all tubes taken together are better described by a Herschel-Bulkley constitutive relation,

$$\sigma = \sigma_y + K\dot{\gamma}^n. \quad (2)$$

The dashed line in Fig. 4 is a fit of the data to Eq. 2 which gives the yield stress  $\sigma_y = 370 \pm 70$  dyn/cm<sup>2</sup>,  $K = 610 \pm 100$  dyn s <sup>$n$</sup> /cm<sup>2</sup>, and  $n = 0.58 \pm 0.09$ . The data were also fit to a Bingham model, for which  $n = 1$ , as shown by the dotted line in Fig. 4. This fit gives  $\sigma_y = 540 \pm 40$  dyn/cm<sup>2</sup> and  $K = 290 \pm 30$  dyn s/cm<sup>2</sup>, but does not describe the combined data as well as the full Herschel-Bulkley expression, particularly at low shear rates.

The time constant  $\tau_a$  over which the drag force builds up to its steady-state value is proportional to  $1/v$  for a given tube size, with the slope depending on  $D/d$ . The data for the different tube sizes again collapse onto a single curve if  $\tau_a$  is plotted against  $\dot{\gamma}^{-1}$ , the reciprocal of the shear rate, as in Fig. 5. Within the scatter,  $\tau_a$  is proportional to  $\dot{\gamma}^{-1}$ ; a fit gives  $\tau_a = (0.23 \pm 0.01)\dot{\gamma}^{-1}$ .  $\dot{\gamma}^{-1}$  is the time it takes for the sphere to move a distance equal to the size of the sheared region surrounding

it, and is therefore the timescale for the initial formation of this sheared region when the sphere starts to move – the drag force builds up as the foam structure within the sheared zone is modified by the motion of the sphere.

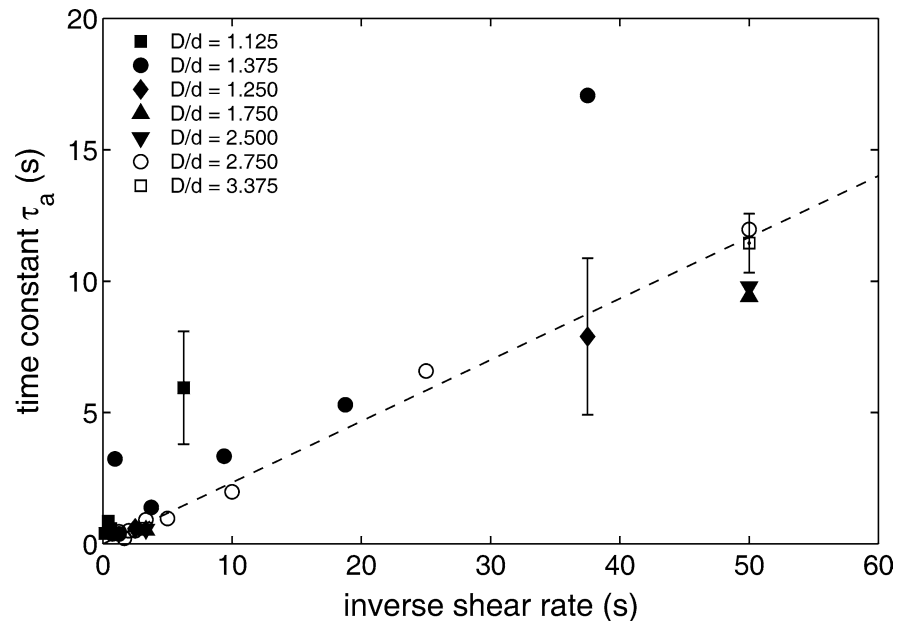
We also analysed the relaxation of the force (or equivalently, the stress) after the motion of the ball was stopped. The graph at the bottom of Fig. 1 shows a portion of the relaxation data from one run, illustrating an initial rapid partial decay of  $F$ , followed by a much slower relaxation of the remaining force. A sum of three exponential decays was needed to describe the relaxation:

$$F(t) = F_b e^{-t/\tau_b} + F_c e^{-t/\tau_c} + F_d e^{-t/\tau_d} + F_1, \quad (3)$$

indicating that three distinct processes contribute to stress relaxation in the foam. A fit to this expression is shown as the dashed line in the graph at the bottom of Fig. 1 (note that the scale on the ordinate of this graph is logarithmic). This expression has seven fitting parameters:  $F_1$  is the residual force after infinite time,  $F_b$ ,  $F_c$ , and  $F_d$  are the amplitudes of the three components, and  $\tau_b$ ,  $\tau_c$ , and  $\tau_d$  are the respective time constants. These parameters were again determined for a range of values of  $v$  and  $D/d$ . The three time constants were well separated in value:  $\tau_b$ , the shortest time, was of order a few seconds,  $\tau_c$  was a few tens of seconds, and  $\tau_d$ , the longest relaxation time, was several hundred seconds. Within the experimental scatter of about 10%,  $F_a = F_b + F_c + F_d$ , so all of the stress induced by the motion of the ball eventually relaxes via the combination of these three processes.

The initial magnitude of the component of the stress that relaxes most quickly,  $\sigma_b$ , is plotted as a function of  $\dot{\gamma}$  in Fig. 6. Note that  $\dot{\gamma}$  is now the shear rate of the flow

**Fig. 5** The time constant  $\tau_a$  for the initial build-up of the drag force as a function of the reciprocal of the shear rate,  $\dot{\gamma}^{-1}$ . The symbols are as in Fig. 4. The error bars indicate the range of data obtained from multiple runs under the same conditions



before the ball stopped moving. We have again converted the force  $F_a$  to a stress assuming the results of Beris et al (1985) discussed above. A power law fit to these data gives  $\sigma_b = (560 \pm 50)\dot{\gamma}^{0.61 \pm 0.04}$ . Both the exponent and the coefficient here are the same, within our uncertainty, as those determined for the Herschel-Bulkley relation fitted to our flow curve data in Fig. 4, so  $\sigma_b$  is equal within error to the steady-state shear-induced stress in excess of the yield stress. This is in accord with expectations: in a yield-stress fluid, the residual stress remaining after relaxation should be the

yield stress, since it is the stress measured at zero shear rate (Magnin and Piau 1990). Here the situation is complicated because the properties of the foam change continuously as it ages, and as noted above, the remaining stress – the  $c$  and  $d$  terms in Eq. 3 – eventually relaxes as well as a result of these changes. The relaxation of the remaining stress takes place over times much longer than  $\tau_b$ , however, so it is reasonable to identify this rapidly-relaxing component of the stress with that in excess of the yield stress, or in other words, the stress due to the viscous component of the force on the sphere.

**Fig. 6** A plot of  $\sigma_b$ , the initial magnitude of the component of the stress that relaxes fastest when the motion of the sphere is stopped, as a function of the shear rate of the previous motion. The dashed line is a power-law fit which gives an exponent of  $0.61 \pm 0.04$

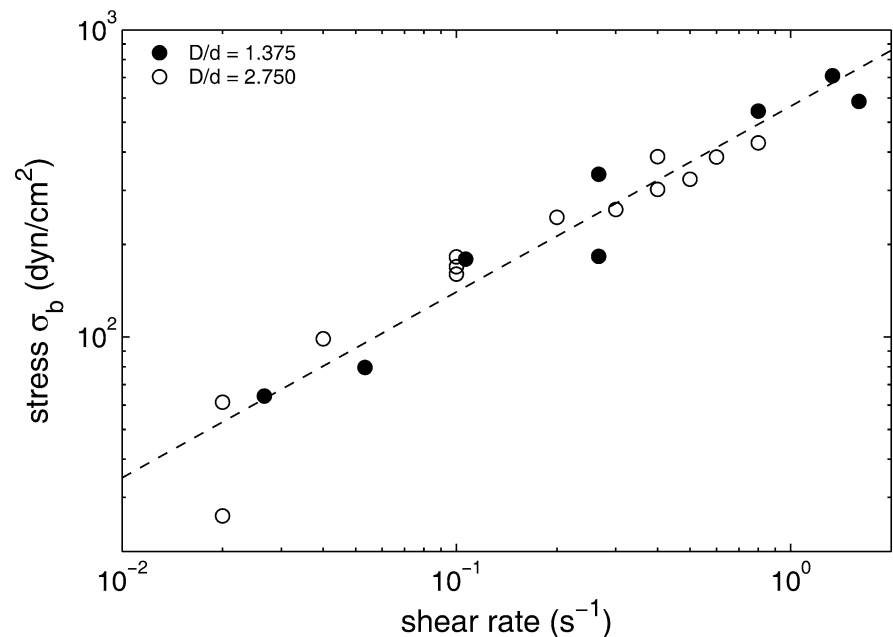
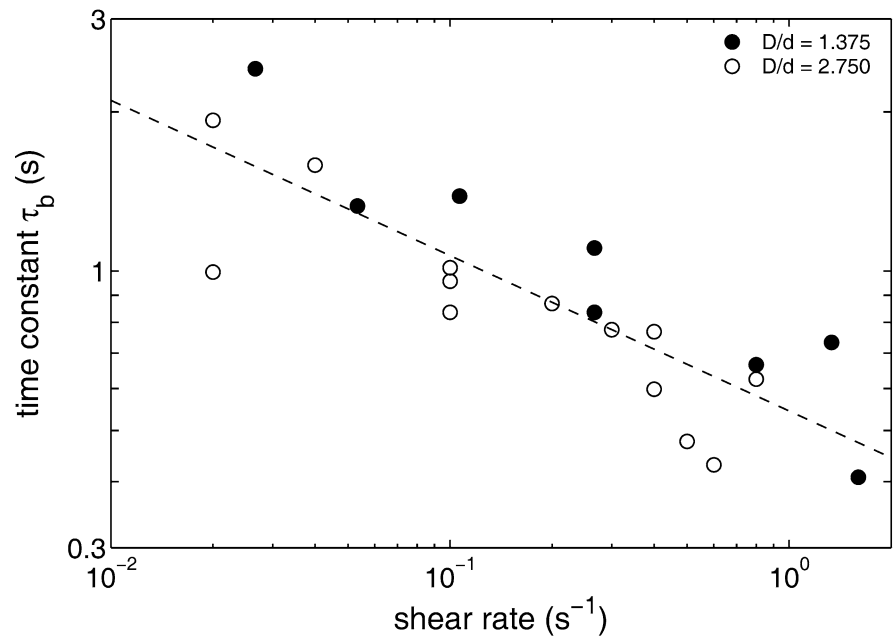


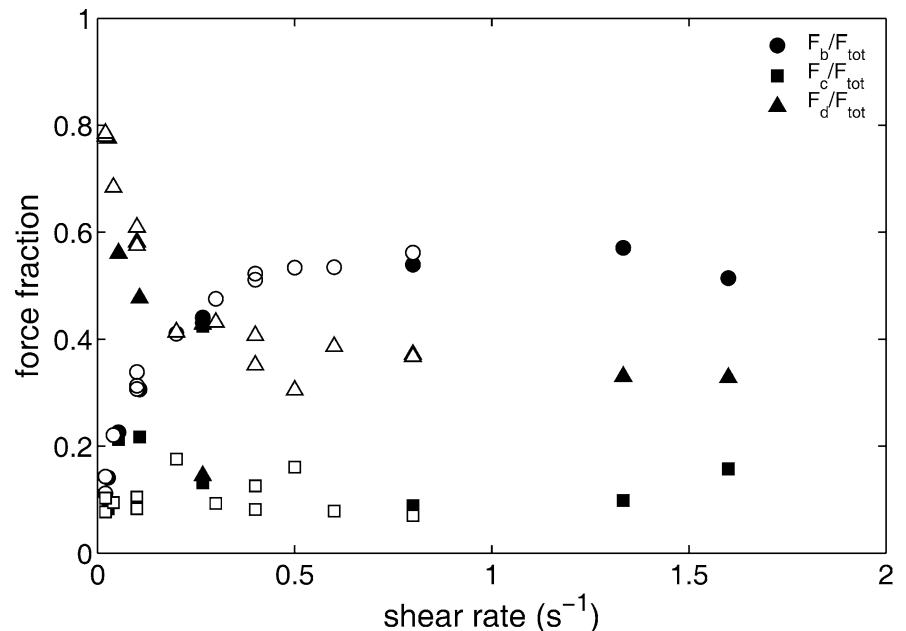
**Fig. 7** A plot of  $\tau_b$ , the shortest of the three time constants for the relaxation of the stress after the motion of the sphere is stopped, plotted as a function of the (previous) strain rate  $\dot{\gamma}$ . This is the time constant for the relaxation of  $\sigma_b$ , which was plotted in Fig. 6. The dashed line is a power law fit with an exponent of  $-0.29 \pm 0.04$



Although the ball is no longer moving, the relaxation time constant  $\tau_b$  of this component of the stress also depends on the shear rate of the past motion.  $\tau_b$  decreases weakly with an increase in the past shear rate, as shown in Fig. 7 for two tube sizes. A power law fit to the two data sets gives  $\tau_b = (0.54 \pm 0.05)\dot{\gamma}^{-0.29 \pm 0.04}$ . The fact that this relaxation depends on the previous shearing of the foam suggests that this component of the stress is released by a relatively rapid restructuring of the foam within the (previously) sheared region immediately surrounding the sphere.

The magnitudes of the other two components of the relaxing force,  $F_c$  and  $F_d$ , show no systematic dependence on speed or tube size, and hence on shear rate, within our experimental scatter. However, the fraction of the total force (or, equivalently, stress) represented by each component of Eq. 3 does vary systematically with the shear rate of the previous motion, as shown in Fig. 8. Here we have plotted  $F_a/F_{tot}$  (circles),  $F_c/F_{tot}$  (squares), and  $F_d/F_{tot}$  (triangles), where  $F_{tot} = F_b + F_c + F_d$  is the sum of the three components of the force. The fraction of the total force due to viscous drag,  $F_b/$

**Fig. 8** The fraction of the total force due to each component in Eq. 3 plotted as a function of the strain rate of the flow before the ball was stopped. Solid symbols are for  $D/d=1.375$  and open symbols are for  $D/d=2.750$



$F_{\text{tot}}$ , increases with shear rate as expected, up to just over 50% of the total force. The fraction due to  $F_c$  remains constant at about 10% of the total, while the fraction due to the third component  $F_d$ , which is the component that relaxes most slowly, is 80% of the total at low shear rates and decreases to about 35% at higher shear rates.

The data for the relaxation time constant  $\tau_c$  are somewhat noisy but indicate a weak decrease as shear rate is increased, from about 30 s (with considerable scatter) for runs at low  $\dot{\gamma}$ , down to 5 s at high  $\dot{\gamma}$ . These times are close to the time of approximately 10 s between local bubble rearrangement events at a given site in the fresh foam, determined in diffusing wave spectroscopy experiments (Durian et al 1991b; Cohen-Addad and Höhler 2001), and so we associate the decay of this component of the stress with relaxation resulting from such events. Our values of  $\tau_d$ , on the other hand, are scattered between 100–900 s and show no systematic dependence on either  $v$  or tube size. This suggests that this longer time is related to ageing of the foam itself and not to a relaxation of the changes induced by the shear.

## Discussion

Flow in a Herschel-Bulkley yield-stress fluid can be characterised by the Oldroyd number

$$Od = \frac{\sigma_y}{K(v/d)^n}. \quad (4)$$

This dimensionless group is the ratio of plastic (yield-stress) effects to viscous effects. Using the values of the parameters  $\sigma_y$ ,  $K$ , and  $n$  obtained from fitting our flow curve (Fig. 4) to the Herschel-Bulkley model, we find  $Od=12.9$  for our lowest pulling speed ( $v=0.0127$  cm/s) and  $Od=1.0$  for our highest ( $v=1.02$  cm/s). Therefore the effects of yield stress are always significant in our experiments, and in most cases dominant.

One can also define a modified Reynolds number (Atapattu et al 1995),

$$Re^* = \frac{v^{2-n} d^n \rho}{K}, \quad (5)$$

where  $\rho$  is the density of the material. Taking the density of the foam to be  $0.08$  g/cm<sup>3</sup> based on its 8% fluid fraction, we find  $Re^*$  to range from  $4.5 \times 10^{-7}$  up to  $2.3 \times 10^{-4}$ , so inertial effects are always small compared to viscous and plastic effects.

In estimating the stress we assumed that the result of Beris et al (1985), which relates the yield stress to the applied force necessary to overcome it, could also be applied to the moving sphere. This assumption is expected to be valid for high  $Od$ , that is, when viscous stresses are much smaller than the yield stress. Our values for the yield stress, the stress during relaxation,

and the stress at low  $\dot{\gamma}$  should therefore be reasonably accurate. On the other hand, our approximation probably overestimates the stress at large shear rates. While a rough calculation suggests that the error could be as high as 40% at  $\dot{\gamma}=1$  s<sup>-1</sup>, the experimentally observed equality of  $\sigma_b$  – measured when the ball is not moving and viscous stresses are zero – and  $\sigma_a - \sigma_y$  – measured at non-zero  $\dot{\gamma}$  – indicates that in fact the error introduced is not large.

Gopal and Durian (1999) estimated  $\sigma_y$  and  $K$  for Gillette Foamy Regular using a Bingham model ( $n=1$  in Eq. 2). They based their estimate on rheological measurements of the elastic modulus and the yield strain, combined with values for the surface tension of the bubbles and the duration of bubble rearrangement events. They found that  $\sigma_y \approx 150$  dyn/cm<sup>2</sup> and  $K \approx 15$  dyn s/cm<sup>2</sup>.  $\sigma_y$  determined in this way is somewhat smaller than the value found from our experiments, although it is of the same order of magnitude.

The drag force on a moving sphere is in general affected by the presence of container walls. For Stokes flows in a Newtonian fluid, the flow field induced by the moving sphere extends out to  $r=\infty$ , and the walls therefore have an effect on the drag force for any container. In experiments similar to those described above but using a viscous Newtonian fluid, we find a continuous variation in the drag force with tube size, in agreement with theoretical predictions (Happel and Brenner 1965). In the present case, however, the drag force is constant for large tubes and increases only when the tube size is below a certain threshold. This is evidence for the presence of a sheared region surrounding the moving sphere, with the foam outside that sheared region remaining unperturbed by the flow. If the sheared region does not extend to the container walls, the walls have no effect on the measured drag force. Our results indicate that the sheared region extends approximately one sphere radius away from the sphere for a pulling speed of 0.381 cm/s; that is, its radial extent measured from the centre of the sphere is  $d$ . The size of the sheared region decreases for lower speeds.

Deglo De Besses et al (2004) numerically determined the extent of the sheared region around a sphere moving through an infinite Herschel-Bulkley fluid as a function of  $Od$ . For  $Od$  between 1 and 10, and assuming no slip at the surface of the ball, they found the radial extent of the fluidised region to vary between 2.5 and 1.5 ball radii, in very good agreement with our experimental results.

The yield stress in a foam is due to the surface tension of the bubbles in the foam, coupled with the fact that the bubbles cannot rearrange themselves easily in response to a small applied stress. When the yield stress is exceeded, the bubbles “un-jam” in the sheared region surrounding the moving sphere, and can flow past each other. The build-up of the force when the sphere starts moving through the foam occurs over a timescale

inversely proportional to the imposed shear rate. This is simply the time over which the sheared region develops in response to the motion of the sphere.

The relaxation of stress when the motion of the sphere is stopped involves three distinct processes, each with a characteristic time constant. The data plotted in Fig. 6 show that the component that relaxes fastest, indicated by the subscript “b” above, is equal within error to that part of the stress that is due to the viscous drag; that is, to the stress in excess of the yield stress. This component is the largest of the three for large shear rates. It relaxes exponentially with a time constant  $\tau_b$ , of order one second, which was shown in Fig. 7 to depend weakly on the shear rate of the previous motion. We interpret this relaxation as being due to an overall bulk relaxation of the foam structure in the previously-sheared region in response to the cessation of motion.

The relaxation of the second component occurs with a time constant  $\tau_c$  which is on the order of 10 s. This time-scale is consistent with that for local (rather than bulk) bubble rearrangement events within the foam. The time between bubble rearrangements at a given point in the absence of shear has been measured using diffusing-wave spectroscopy. For fresh foam, Durian et al (1991b) found a value of approximately 10 s, while Cohen-Addad and Höhler (2001) found 6 s; these times increased as the foam aged. We therefore associate  $\tau_c$  with the relaxation of stress due to these local events. This process is responsible for relaxing most of the stress at low shear rates, and remains significant even at the highest shear rates.

Finally, the time constant  $\tau_d$  characterising the slowest contribution to the relaxation is of order a few hundred seconds. This is much slower than the rate of local bubble rearrangements, and we associate this with a “creep” process resulting from slow changes in the characteristics of the foam, or in other words from foam aging. This process relaxes roughly 10% of the stress at all shear rates. Durian et al (1991b) showed that the mean bubble size in this foam remained roughly constant until the foam’s age was approximately 1200 s, after which the bubble size grew like a power law in time.

This power-law behaviour implies that there is in fact no characteristic timescale for coarsening in this scaling regime. Our experiments take place at earlier times, however, when, although their mean size does not change, the size distribution of the bubbles evolves as gas diffuses from smaller, high-pressure bubbles into larger, lower-pressure bubbles. This evolution in the size distribution results in the relaxation of the stress observed in our experiments.

## Conclusions

We have measured the steady state force on a sphere moving at constant speed through an aqueous foam, as well as the build-up and relaxation of this force when the motion is started and stopped, respectively. The foam behaves as a yield-stress fluid, and our results for the dependence of the drag force on container size are in agreement with the presence of a sheared region surrounding the moving sphere – wall effects are not present unless this sheared region reaches to the wall of the container. From our steady-state drag measurements, we estimate a flow curve for the foam, which is well described by a Herschel-Bulkley law with a yield stress of  $270 \pm 70$  dyn/cm<sup>2</sup>. The transient build-up of the drag force is well described by a single exponential approach to the steady state force, with a time constant proportional to the reciprocal of the shear rate. The relaxation of the force after the motion stops, however, requires a sum of three separate exponential decay processes for an adequate description. We identify these processes, in order of increasing time constant, with bulk relaxation of the foam structure in the sheared region, local bubble rearrangements, and overall ageing of the foam.

**Acknowledgements** This research was supported by NSERC of Canada and CNRS, France. I am grateful to D. Durian, P. Chafe and A. Walsh for helpful discussions, and K. Burfitt for assistance with preliminary experiments.

## References

- Atapattu DD, Chhabra RP, Uhlherr PHT (1990) Wall effect for spheres falling at small Reynolds number in a viscoplastic medium. *J Non-Newton Fluid Mech* 38:31–42
- Atapattu DD, Chhabra RP, Uhlherr PHT (1995) Creeping sphere motion in Herschel-Bulkley fluids: flow field and drag. *J Non-Newton Fluid Mech* 59:245–265
- Beaulne M, Mitsoulis E (1997) Creeping motion of a sphere in tubes filled with Herschel-Bulkley fluids. *J Non-Newton Fluid Mech* 72:55–71
- Beris AN, Tsamopoulos JA, Armstrong RC, Brown RA (1985) Creeping motion of a sphere through a Bingham plastic. *J Fluid Mech* 158:219–244
- Blackery J, Mitsoulis E (1997) Creeping motion of a sphere in tubes filled with a Bingham plastic material. *J Non-Newtonian Fluid Mech* 70:59–77
- Bolton F, Weaire D (1990) Rigidity loss transition in a disordered 2D froth. *Phys Rev Lett* 65:3449–3451
- Cohen-Addad S, Höhler R (2001) Bubble dynamics relaxation in aqueous foam probed by multispeckle diffusing-wave spectroscopy. *Phys Rev Lett* 86:4700–4703
- Deglo De Besses B, Magnin A, Jay P (2004) Sphere drag in a viscoplastic fluid. *AIChE J* (to be published)

- Durian DJ (1995) Foam mechanics at the bubble scale. *Phys Rev Lett* 75:4780–4783
- Durian DJ (1997) Bubble-scale model of foam mechanics: Melting, nonlinear behavior, and avalanches. *Phys Rev E* 55:1739–1751
- Durian DJ, Weitz DA, Pine DJ (1991a) Multiple light-scattering probes of foam structure and dynamics. *Science* 252:686–688
- Durian DJ, Weitz DA, Pine DJ (1991b) Scaling behavior in shaving cream. *Phys Rev A* 44:R7902–R7905
- Gopal AD, Durian DJ (1995) Nonlinear bubble dynamics in a slowly driven foam. *Phys Rev Lett* 75:2610–2613
- Gopal AD, Durian DJ (1999) Shear-induced “melting” of an aqueous foam. *J Colloid Interf Sci* 213:169–178
- Gopal AD, Durian DJ (2003) Relaxing in foam. *Phys Rev Lett* 91:188–303
- Happel J, Brenner H (1965) *Low Reynolds number hydrodynamics*. Prentice Hall, Englewood Cliffs, NJ
- Hariharaputhiran M, Subramanian RS, Campbell GA, Chhabra RP (1998) The settling of spheres in a viscoplastic fluid. *J Non-Newton Fluid Mech* 79:87–97
- Heller JP, Kuntamukkula MS (1987) Critical review of the foam rheology literature. *Ind Eng Chem Res* 26:318–325
- Jossic L, Magnin A (2001) Drag and stability of objects in a yield stress fluid. *AIChE J* 47:2666–2672
- Kabla A, Debrégeas G (2003) Local stress relaxation and shear banding in a dry foam under shear. *Phys Rev Lett* 90:258303
- Khan SA, Armstrong RC (1986) Rheology of foams: I. Theory for dry foams. *J Non-Newton Fluid Mech* 22:1–22
- Kraynik AM (1988) Foam flows. *Annu Rev Fluid Mech* 20:325–357
- Magnin A, Piau JM (1990) Cone and plate rheometry of fluids with a yield stress. *J Non-Newton Fluid Mech* 36:85–92
- Ozokuno T, Kawasaki K (1995) Intermittent flow behavior of random foams: A computer experiment on foam rheology. *Phys Rev E* 51:1246–1253
- Princen HM (1983) Rheology of foams and highly concentrated emulsions I: Elastic properties and yield stress of a cylindrical model system. *J Colloid Interf Sci* 91:160–175
- Reinelt DA, Kraynik AM (1990) On the shearing flow of foams and concentrated emulsions. *J Fluid Mech* 215:431–455
- Tewari S, Schiemann D, Durian DJ, Knobler CM, Langer SA, Liu AJ (1999) Statistics of shear-induced rearrangements in a model foam. *Phys Rev E* 60:4385–4396
- Weaire D, Hutzler S (2001) *The physics of foams*. Oxford University Press, Oxford, UK